Regression Rate Considerations in Hybrid Rocket Propulsion

Max Kandula, Ph.D.
Technical Fellow, KBR
Space Coast Engineering & Sciences Group
5095 S Washington Av, Suite 202
Titusville, FL 32780

A brief review of hybrid rocket engines is provided with regard to combustion and solid fuel regression rates. Methods of enhancing regression rates in hybrids are presented with reference to the role of metal nanoparticles embedded into the solid propellant, including particle size and particle loading. The physical nature of the combustion of metal particles is described. System variables influencing the regression rates have been discussed with regard to design and scaling considerations. The role of radiation of heat from the metal particles to the propellant surface requires further investigations.

1. Introduction

In recent years, there is growing interest in the development of hybrid rocket engines for space propulsion. Hybrid rockets are suitable alternatives to conventional rockets for various space applications, such as first-stage boosters, sounding rockets, upper-stage vehicles, etc.

A typical schematic (layout) of the hybrid rocket propulsion system is presented in **Fig**. 1(Eilers et al., 2008). Hybrid chemical rockets store fuel and oxidizer separately. The system consists of pressurizing gas tank, pressure regulator, liquid oxidizer tank, combustion chamber with solid propellant core, and nozzle. Liquid oxidizer is injected into a cylindrical chamber enclosing the solid propellant, with the combustion gases expelled through the nozzle.

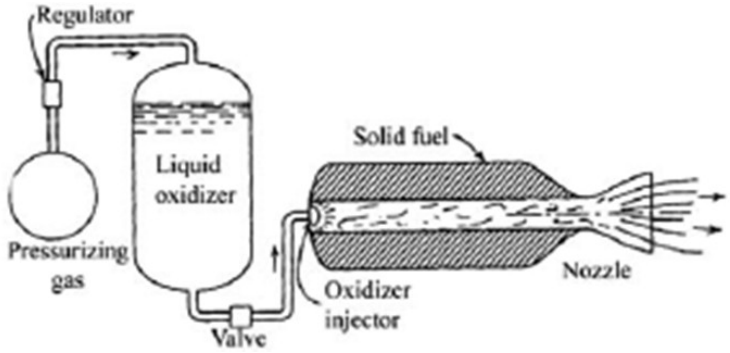

Fig. 1 Schematic of a hybrid rocket propulsion system (Eilers et al., 2008).

In a hybrid rocket motor, the solid propellant is cast into the combustion chamber with suitable grain geometry (**Fig**. 2; Calabro, 2011). Combustion of the solid fuel surface is initiated by an ignitor with sufficient energy, and sustained combustion fuel takes place by the vaporization of injected liquid oxidizer. Combustion of the propellants takes place in the boundary layer by the diffusion of the vaporized fuel and oxidizer forming the diffusion flame (Estey and Hughes, 1992). A precombustion chamber is used to mix the oxidizer, and a post combustion chamber is utilized to mix the combustion products prior to expansion in the nozzle. Due to strong recirculation in the pre-combustion chamber, stable combustion is expected (Calbro, 2011).

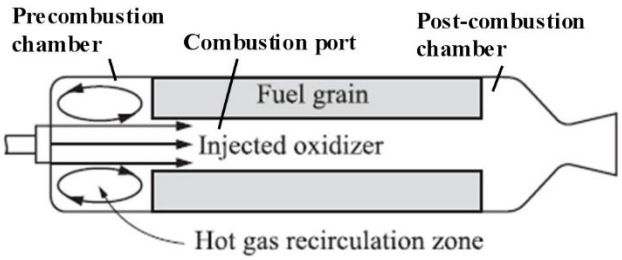

Fig. 2 Hybrid rocket combustion chamber and nozzle (Calabro, 2011).

2. Comparison of Hybrid Rocket Engines with Solid and Liquid Rocket Engines

Hybrid rockets offer several advantages relative to traditional solid and liquid rocket engines (Marquardt and Majdalani, 2020). The physical separation of the fuel and oxidizer in hybrids leads to diffusion-limited and less-efficient combustion as compared to the quasi-premixed flame observed in solid and liquid rocket engines (Marquardt, 2020). Hybrid rocket engines yield specific impulse values between that of solid and liquids, but produce specific impulse values offered by liquid engines when properly designed. Hybrids also offer safety advantages during all phases of their life cycle such as fabrication, storage and handling because the propellants are generally non-toxic and inert until mixed and heated in the combustion chamber.

Hybrids are less complex and therefore less costly than liquid rockets because hybrids require considerably less plumbing and turbomachinery. Relative to liquid rocket engines, hybrids provide safety from explosion hazard due to phase-separation among propellants. Hybrids provide simpler engine design, greater flexibility in oxidizer-fuel selection with minimum environmental effects.

Relative to solid rockets, hybrids offer flexible throttling and facilitate non-destructive aborts (on-demand thrust termination/restart or thrust tailoring) unlike solid rockets. Hybrid rockets were found to be relatively insensitive to cracks in the fuel grain, making hybrids an attractive alternative to solid rocket boosters. Hybrid fuels include reduced debonding and crack sensitivity (diffusion-controlled combustion), fuel insensitivity to combustion instability and increased specific impulse relative to solid rockets (Akhtar and Hassan, 2018).

Hybrids have limitations such as low fuel regression rates, and varying mixture ratio (O/F) during combustion (Akhtar and Hassan, 2018); the low regression of polymeric fuels and poor combustion efficiency is largely attributed to the diffusion-flame-limited combustion in hybrid rocket engines (Aktar and Hassam, 2018).

3. Typical Fuel-Oxidizer Combinations for Hybrid Rocket Engines

The theoretical performance of various fuel-oxidizer combinations used in hybrid rocket propulsion is presented in Table 1(Calabro, 2011; Kuo and Chiaverini, 2007), along with the optimum O/F ratio, specific impulse I_{sp}, and the characteristic velocity c^*.

Table 1. Theoretical performance of various fuel/oxidizer combinations in hybrid rocket engines (p_c =3.5 Mpa, p_e =0.1 MPa).

Propellant Combination	Opt. O/F	I_{sp} (s)	c* (m/s)
HPTB/LOX	1.9	280	1820
HPTB/N2O	7.1	247	1604
HPTB/N2O4	3.5	258	1663
HPTB+Al(40%)/LOX	1.1	274	1757
PMM/LOX	1.5	259	1661
Paraffin/LOX	2.5	281	1804
Paraffin/N2O	8	248	1667

One of the challenges in the design of a hybrid motor is to select a fuel grain design that results in an average O/F ratio near optimum. **Figure 3** presents the calculated adiabatic flame temperature and characteristic velocity for HPTB and nitrous oxide as a function of oxidizer-to-fuel (O/F) ratio for various chamber pressures. The calculations were made with the id of the NASA's CEA (Chemical Equilibrium with Applications) code (Gordon and McBride, 1994) which calculates the thermodynamic and transport properties of the products of combustion. For O/F less than about 4, the adiabatic temperature and the characteristic velocity seem to be independent of chamber pressure. The peak values of adiabatic flame temperature and the characteristic velocity occur in the range of O/F about 5 and 6.

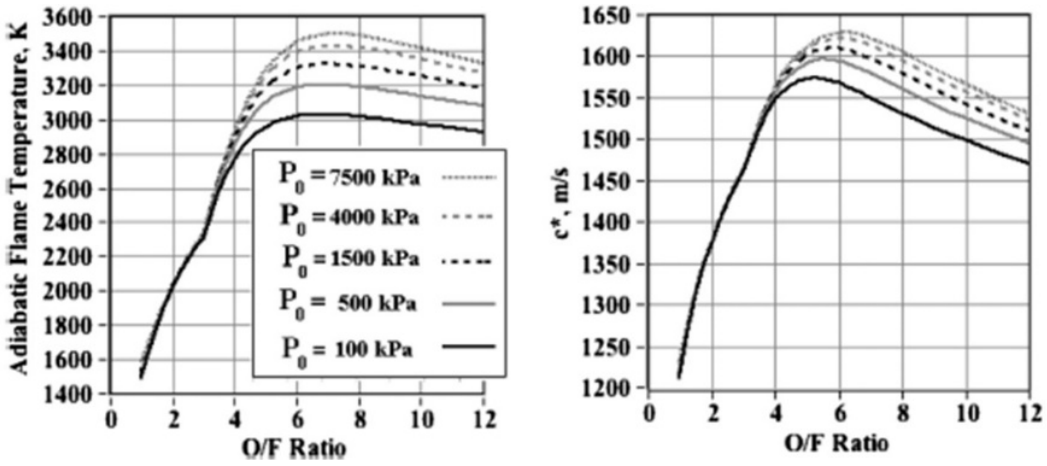

Fig. 3 Adiabatic flame temperature and characteristic velocity for HPTB/N2O combustion (Whitmore et al., 2013).

Figure 4 displays the theoretical performance of metallized HPTB fuel with 20% aluminum loading with various oxidizers (Estey and Whiting hall, 1992). Because of metal oxides in the combustion products there is an increase in the radiative heat transfer and a higher fuel regression rate.

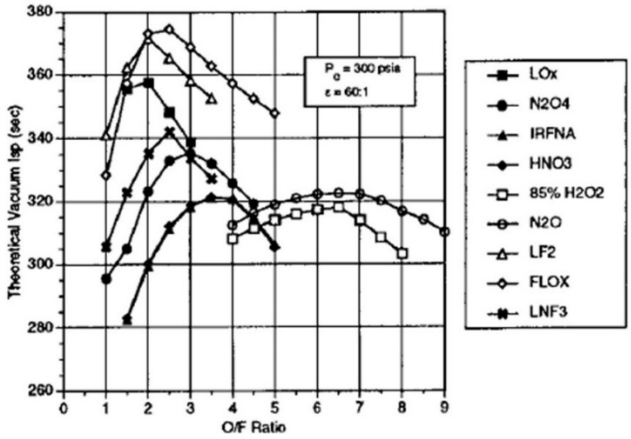

Fig. 4 Theoretical performance of HPTB with 20% aluminum loading for various oxidizers (Estey and Hughes, 1992).

4. Combustion Processes in Hybrid Rockets

4.1 Boundary Layer Combustion (Diffusion Flame)

The combustor of hybrid rockets entails fluid dynamic, chemical and thermal processes, as the liquid propellant is injected into the combustion chamber (**Fig**. 5; Marquardt, Majdalani, 2020). A turbulent boundary layer forms on the solid fuel grain. Upon ignition, a flame **zone** develops when the fuel and oxidizer mix, with the combustion products flowing axially (and radially) along the length of the combustor. The equilibrium combustion temperature depends on oxidizer-to-fuel ratio, with the fuel flow rate governed by the fuel regression rate.

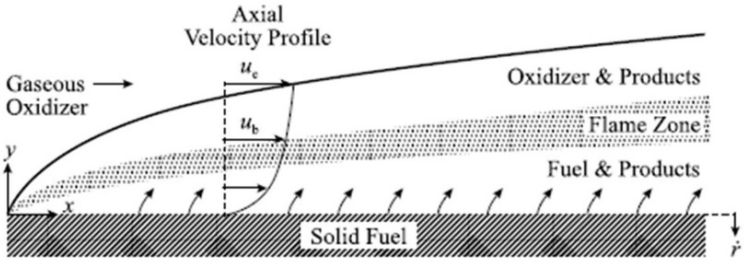

Fig. 5 Schematic of diffusive combustion process in hybrid rocket thrust chambers.

The energy balance in a hybrid rocket combustion chamber is depicted in **Fig.** 6 (Cai et al., 2013). Heat flow from the combustion gases to the fuel surface occurs by turbulent convection and thermal radiation. There is reradiation from the fuel surface back to the combustion chamber, and heat release from the propellant surface due to phase transformation. The surface regression rate is dependent in a complex way on the net energy exchange at the propellant surface. The velocity (U) and temperature (T) distributions in the combusting boundary layer are qualitatively shown. The quantity Q_{conv} refers to convective heat transfer, Q_{rad} refers to radiation heat transfer, and Q_{phase} refers to heat transfer due to phase transformation. The positive sign refers to heat flow from the propellant surface, and the negative sign refers to heat flow into the propellant surface.

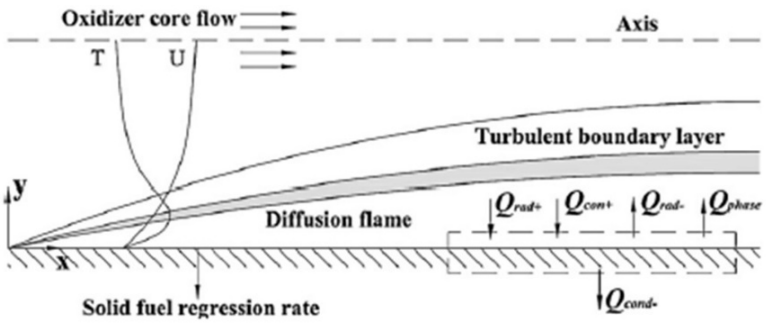

Fig. 6 Representation of energy balance in hybrid rocket combustion chamber (Cai et al., 2013).

4.2 **Enhancement of Fuel Regression Rates**

In view of the importance of the regression rate, several methods have been tested to increase regression rates: fuel grain geometry changes, addition of nano-metal particles to the solid propellant, and swirl injection. The regression rate $\dot{r}$ is defined by the following expression for the fuel mass flow rate m_f :

$$\dot{m}_f = A_p \rho_f \dot{r} \tag{1}$$

where A_p is the port area, ρ_f is the fuel density. The oxidizer mass flow rate $\dot{m}_o$ is computed from the relation

$$\dot{m}_o = A_{\text{inj}} C_d \sqrt{2\rho_o \left(p_0 - p_c \right)} \tag{2}$$

where A_{inj} is the inject C_d or area, is the discharge coefficient, ρ_{ox} is the oxidizer density, p_{ox} is the oxidizer pressure upstream of the injector, and p_c is the chamber pressure. The oxidizer to fuel ratio O/F is given by

$$\text{O/F} = \dot{m}_o / \dot{m}_f \tag{3}$$

The total heat transferred from the combustion products to the fuel surface, $\dot{q}$, is related to the fuel regression rate according to (Eilers and Whitmore, 2008)

$$\dot{q} = \rho_f \dot{r} h_v \tag{4}$$

where h_v is the heat of vaporization of the propellant. The total heat transfer is comprised of both turbulent convection heat transfer $\dot{q}_c$ and radiation heat transfer (gas and particles) $\dot{q}_r$:

$$\dot{q} = \dot{q}_c + \dot{q}_r \tag{5}$$

The convection heat transfer, proportional to the temperature difference between the gas and fuel surface and the oxidizer mass flux is well described, the calculation methods for radiation from the combustion gases and the metal particles require further investigation.

4.2.1 Fuel Grain Geometry

One of the established methods for increasing the regression rate in hybrid rockets is by increasing the fuel surface area exposed to combustion. This is achieved either by shaping the internal fuel port (**Fig. 7a**) or employing multi-port fuel grain (**Fig. 7b**) (Surmacz and Rarata, 2009). The chief disdvantages of this approach is complicated fuel casing (preparation), oxidizer distribution into individual ports, and poor fuel grain integrity (especially near burnout).

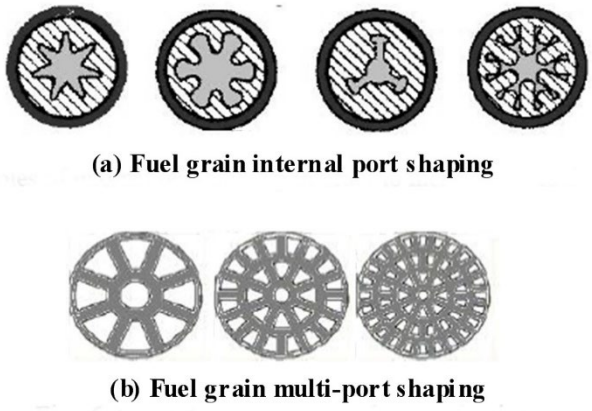

Fig. 7 Methods of enhancement of regression by increasing fuel surface area (Surmacz and Rarata, 2009).

4.2.2 Mechanisms of Nano- Metal Particle Combustion

Metal particles are attractive fuel candidates for various propulsion applications. Aluminum is popular because of its high energy-density, relative safety, and low cost (Sundaram et al., 2016). Nascent Aluminum particles react spontaneously in oxidizing environments, resulting in the formation of amorphous oxide (Al2O3) layer of thickness in the range of 2-4 nm. Nanomaterials have unique and favorable physicochemical properties owing to the presence of large percentage of atoms on the surface, with the percentage of surface atoms increasing from 2% to 92% when the particle size decreases form 100 to 1 nm. Surface toms have higher energy than the interior atoms, resulting in properties size-dependent and substantially different from those of the bulk materials. A general theory of ignition and combustion of nano- and micron-sized aluminum particles has been provided by Sundaram et al. (2016).

The combustion characteristics of nanoaluminum particles are substantially different from those of micron-sized particles (see **Fig. 8a**; Sundaram et al., 2016). The measured flame temperatures are found to be substantially lower than the adiabatic counterparts of the adiabatic counterparts. The aluminum particle is covered by an amorphous oxide layer ($Al2O_3$). The melting temperature of the aluminum particles varies from 473 K at 2 nm to 933 K at 10 nm, and that of the oxide shell in the range of 986 to 1313 K. These are substantially lower than the bulk melting point of 2350 K for the oxide layer. Heat transfer between the particle and the ambient gas occurs by conduction and radiation, with the free molecular effects confined to the so-called Knudsen layer.

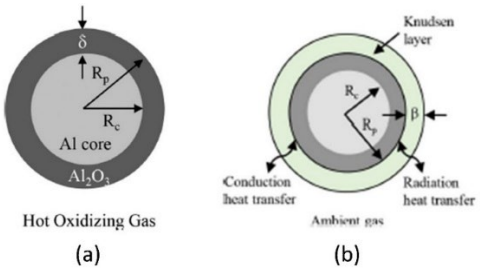

Fig. 8 A passivated aluminum particle in hot combusting gas (Sundaram et al., 2016).

According to Sundaram et al. (2016), the oxidation and combustion of aluminum particles occurs in three stages (**Fig**. 9). In stage (a), the particle is heated to the melting point of the aluminum core. The key mechanisms are heat and mass transfer from the surrounding gas to the particle, and heat and mass diffusion inside the particle. In stage (b), melting is followed by phase transformation in the oxide layer, fracture of oxide layer, mass diffusion in the oxide layer, and heterogamous chemical reactions. In stage (3), oxidizing gas diffuses to the particle surface, followed by mass diffusion across the oxide layer, chemical reactions between aluminum and oxidizing gas (formation of alundum oxide particle), and heat and mass exchange between the particle and the ambient gas. The particle temperature increases gradually approaches the bulk melting temperature of the oxide layer (2350 K). The mode of combustion

(vapor phase vs. surface combustion) depends on the particle size, pressure, and type of oxidizer. Results of CEA analysis suggests that vapor phase reactions occur in oxygenated environments for nonaluminum particles.

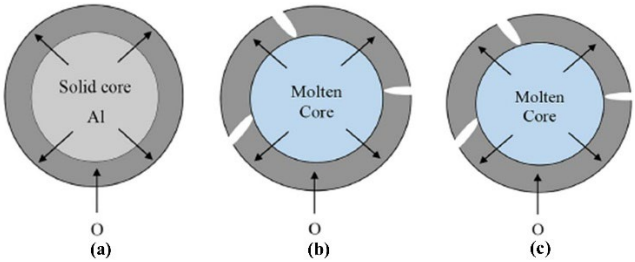

Fig. 9 Main stages of oxidation of nonaluminum particles (Sundaram et al., 2016).

Metal nanoparticles undergo exothermic oxidation, thereby enhancing heat transfer to the fuel surface (Akhtar and Hassan, 2018). The enhancement of in the regression rate of fuels was observed to be significantly higher (350% to 450%) relative to the conventional HPTB based hybrid fuels (paraffin).

4.2.3 Vortex Oxidizer Injection

Another method of enhancing regression rates in hybrid rockets is by swirl injection. Swirl injection has been considered by many investigators, who showed that swirl injection enhances fuel regression rates. Experiments of Knuth et al. (2002) with HPTB/GOX hybrid rockets with vortex injection show that regression rates as much as seven times those in the classical hybrid rockets were realized. **Figure 10** displays the tangential injection section considered by Heydariet al. (2017). Both regression rates and combustion efficiency were increased using swirl injection.

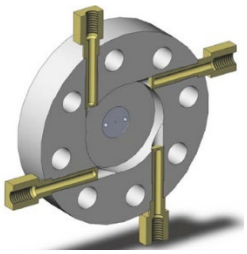

Fig. 10 Sectional view of tangential oxidizer injection (Heydari et al., 2017).

5. Parametric Effects on Fuel Regression Rates

5.1 Influence of Propellant Mass Flux

Figure 11 shows the general influence of mass flux G on regression rates in hybrid motors (as taken form Pistrone, 2012). Three different regions are identified. For medium (intermediate) values of mass flux, the regression rate is diffusion dominated (convective heat transfer from the combustion gases to the nozzle wall). For high values of G, the combustion appears to be controlled by chemical kinetic. Consequently, regression rate becomes pressure dependent. At low values of G, the convective heat transfer diminishes, and radiation form gaseous species may play a significant role. As a result, the regression rate increases depending on the partial pressure of dominant emitting species and port diameter. In this limit, a lower bound of the mass flux is manifested. As the regression rate is relatively small, the fuel tends to remain in the thermal layer of the propellant grain for a long time, and the solid fuel may be cooked/melt underneath the grain surface. Thus, if the mass flux is too low (such as occurs in hybrid rocket engine operation with blowdown systems), chuffing instability may be produced by the perpetual repeating mechanical removal of this soft layer (Pistrone, 2012).

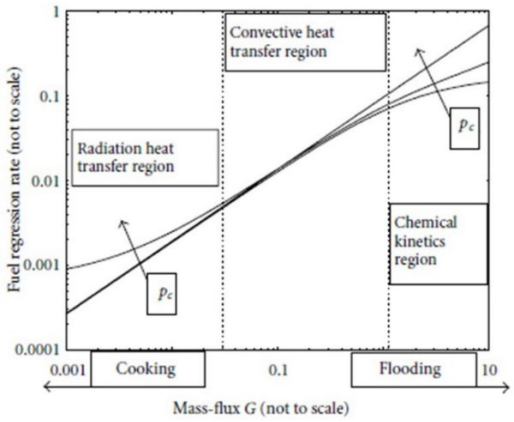

Fig. 11 Dependence of regression rate behavior on oxidizer mass flux.

Figure 12 shows the measurements of Chiaverini et al. (2007) for the regression rates as a function of oxidizer mass flux (see Marquardt ad Majdalani, 2019, 2020; Durand et al., 19xx). Test 15 was performed at a higher pressure than Test 17. The pressure effects on fuel regression rates in the low mass flux region are evidenced, since higher pressure leads to larger regression rates as a result of radiation heat flux. Without radiation, the fuel regression would follow the theoretically derived linear trend considering only turbulent convective heat transfer governing the fuel regression rate. Both data sets agree with the theory at higher mass flux, where convective heat transfer dominates the regression rate.

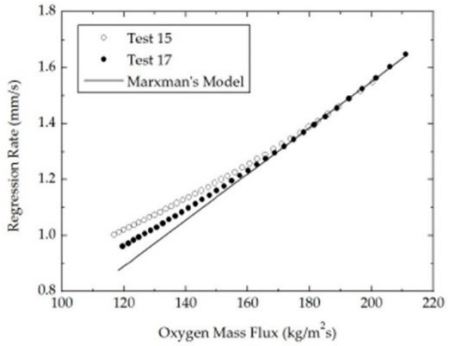

Fig. 12 Dependence of regression rate behavior on oxidizer mass flux.

Figure 13 displays the experimental data of Wooldridge and Muzzy (1967) on regression rate as a function of oxidizer mass flux for GOX/PMMA hybrid rocket motors with three different fuel port diameters (see Cai et al., 2013). The measurements revel that the regression rate increases with oxidizer mass flux and decreases with the fuel port diameter. Also note that, as the fuel port diameter increases, the oxidizer mass flux decreases.

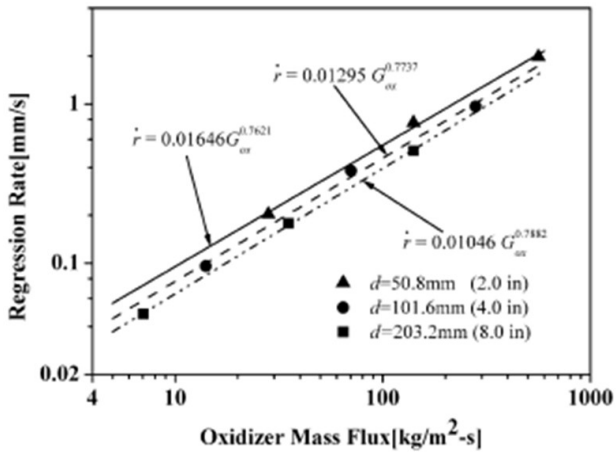

Fig. 13 Dependence of regression rate behavior on oxidizer mass flux.

5.2 Influence of Port Diameter

Measurements by Woolridge and Muzzy (1967), as adapted from Gany (1996), for the dependence of regression rate on the port diameter are displayed in **Fig**. 14 for GOX+PMM system. The quantity G refers to the total mass flux, and D is the port diameter. Both the theory and the data show that the regression rate varies (scales) inversely with the port diameter for various GD levels.

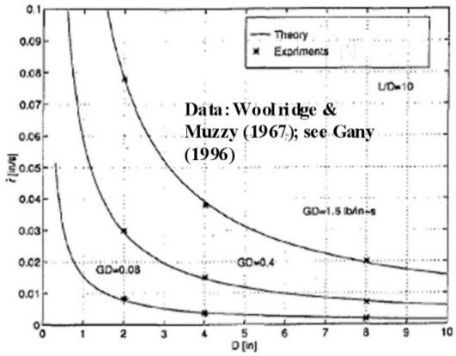

Fig. 14 Dependence of regression rate on the port diameter.

5.3 Influence of Particle Diameter

Figure 15 shows the influence of aluminum particle size on the regression rates of ammonium perchlorate-aluminum particles, according to the data presented in Armstrong et al. (2003). The data show that at the ambient pressure, substantial enhancement of the burn rate occurred as the particle size is reduced from 200 nm to 40 nm. The results also show that the burn rate increases from about 12 to about 580 mm/s for a pressure increase from 0.14 to 15 MPa.

The inverse square law for the regression rate dependence on aluminum particle size is expected at very small particle size on account of the energy release rate determined by the particle surface area, say, specified by the number of Al particles per unit surface area (Armstrong et al., 2003).

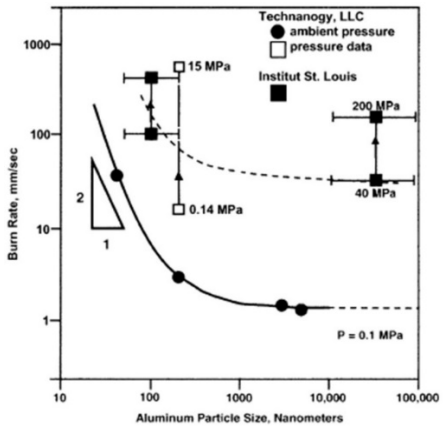

Fig. 15 Dependence of regression rate on the aluminum particle diameter.

5.4 Influence of System Pressure

Measurements by Galfetti et al. (2004), as shown in **Fig. 16**, indicate that the high reactivity of nanoaluminum powders (particles) offers efficient way to increase the regression rate, thereby enhancing the rocket propulsion performance. The influence of system pressure on regression rate is generally expressed by the so-called Vielle's power law (see Baschung et al., 2001)

$$r = \alpha p^{\beta} \tag{1}$$

where α, β are constants to be determined by experiment (Armstrong et a., 2003). Typical value of β is of the order of 0.8 for aluminized propellants.

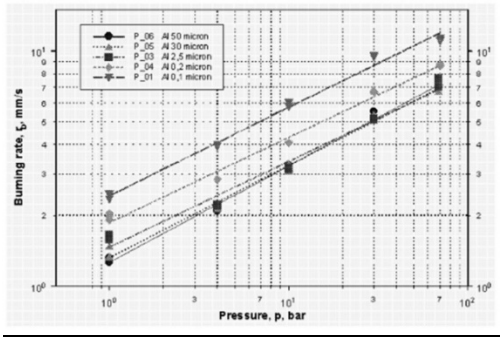

Fig. 16 Dependence of regression rate as a function of pressure for various particle sizes.

5.5 Influence of Swirl

Swirl injection is found to be one of the most efficient means to increase the regression rate of a solid fuel. Data by Gomes et al. (2015) show that at the same oxidizer mass flux, swirl injection increases the regression rate relative to axial injection. Detailed experiments and numerical investigations (CFD) of swirl injection have been reported by Bellomo et al. (2013). Fig. 17 presents the measurements of regression rates with and without swirl injection. Tangential injection of oxidizer increases the regression rates relative to axial injection. The influence of swirl on the regression rate is seen to increase with increasing oxidizer mass flux.

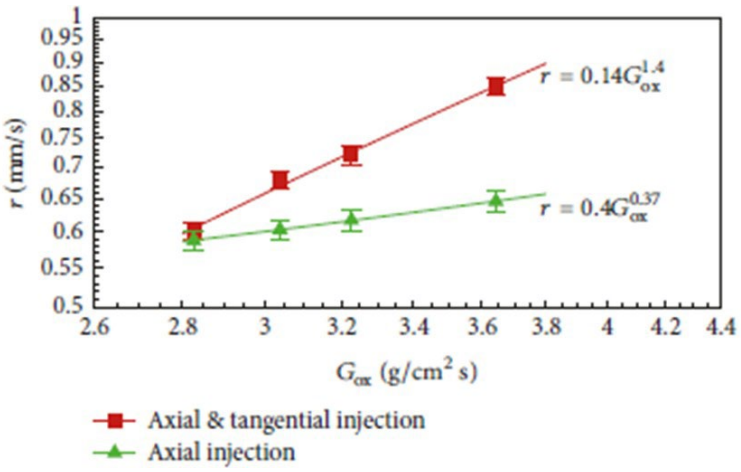

Fig. 17 Dependence of regression rate on the aluminum particle diameter.

7. Conclusions

A brief review on the combustion and regression characteristic of hybrid rocket engines has been presented. Regression rate behavior with regard to various physical parameters has been discussed: propellant mass flux, port diameter, particle diameter, system pressure, and swirl. The results will be helpful in the scaling of hybrid rocket engines.

Acknowledgments

Thanks are due to Donald Jennings, Program Manager, Space Coast Engineering and Sciences Group, KBR, for a review of the manuscript.

References

Akhter, Md. Z., and Hassan, M.A., Characterization of paraffin-based hybrid rocket fuels loaded with nano-additives, J. Experimental Nanoscience, Vol. 13, No. S1, pp. 531-544, 2018.

Armstrong, R.W., Baschung, B., Booth, D.W., and Samirant, M., Enhanced propellant combustion with nanoparticles, Nanoletters (American Chemical Society), Vol. 3, No. 2, pp. 253-255, 2003.

Baschung, B., Grune, D., Licht, H..H., Samirant, M., in Combustion of Energetic Materials; eds. K.K. Kuo, L.T. Deluca, Begell House, New York, p. 219, 2001.

Boardman, T.A., Hybrid propellant rockets, in G.P. Sutton, O. Niblarz (Eds.), Rocket Propulsion Elements, 7th ed., New York, 2001, pp. 579-607.

Bellomo, N., Barato, F., Faneza, M., Lazzarin, M., Bettella, A., and Pavarin, D., Numerical and experimental investigation of unidirectional vortex injection in hybrid rocket engines, J. Propulsion and Power, Vol. 29, No. 5, pp. 1097-1113, September-October 2013.

Calabro, M., Overview on hybrid propulsion, Progress in Propulsion Physics, Vol. 2, pp. 353-374, 2011.

Cai, G., Zeng, P., Li, X., Tian, H., and Yu, N., Scale effect of fuel regression rate in hybrid rocket motor, Aerospace Science and Technology, Vol. 24, pp. 141-146, 2013.

Chiaverini, M., and Kuo, K.K., Fundamentals of hybrid rocket combustion and propulsion , Progress in Aeronautics and Astronautics, AIAA J., Vol. 218, pp. 104, 2007.

Durand, , J-E., Raynaud, F., Lamet, J-M, Tesse, L., Lestrade, J-Y, Numerical study of regression in hybrid rocket engine, AIAA Propulsion and Energy 2018, July 2018.

Eilers, S.D., and Whitmore, S.A., Correlation of hybrid rocket propellant regression measurements with enthalpy-balance model predictions, J. Spacecraft and Rockets, Vol. 45, No. 5, September-October, 2008.

Estey, P.N., and Hughes, B.G.R., The opportunity for hybrid rocket motors in commercial space, AIAA-92-3431, AIAA/SAE/ASME/ASEE 28th Joint Propulsion Conference and Exit, July 26-28, 1992, Nashville, TN.

Galfetti, L., Severini, F., De Luca, L.T., and Meda, L., Nono-propellants for space propulsion, Proc. 4th Int. Spacecraft Propulsion Conference, Cagliari, Sardinia, Italy, 2-4 June 2004 (ESA SP-555, October 2004).

Gany, A., Scale effects in hybrid rocket motors under similarity conditions, AIAA-96-2846, 1996.

Gomes S.R., Rocco, L., and Rocco, J.A.F.F., Swirl injection on hybrid rocket motors, J. Aerosp. Technol. Manag., Vol. 7, No. 4, pp. 418-424, 2015.

Gordon, S., and McBride, B.J., Computer program for calculation of complex chemical equilibrium compositions and applications, NASA RP-1311, 1994.

Heydari, M.M., and Massoom, N.G., Experimental study of the swirling oxidizer flow in HPTB/N2O hybrid rocket motor, Int. J. Aerospace Engineering, Vol. 2017, Article ID 3174140, 2017.

Knuth, W.H., Chiaverini, M.J., Sauer, J.A., and Gramer, D.J., Solid-fuel regression rate behavior of vortex hybrid rocket engines, J. Propulsion and Power, Vol. 18, No. 3, pp. 600-609, 2002.

Kodson, F.J., and Williams, F.A., Pressure dependence of non-metallized hybrid fuel regression rates, AIAA J., Vol. 5, No. 4, pp. 774-778, 1967.

Kuo, K.K., and Chiaverini eds., Fundamentals of Hybrid Rocket Combustion and Propulsion, Progress in Astronautics and Aeronautics Ser., p. 218, Resaton, VA, 2007.

Marquardt, T., and Majdalani, J., Review of classical diffusion-limited regression rate models in hybrid rockets, Aerospace, Vol. 6, 75, 2019.

Marquardt, T.A., and Majdalani, J., A primer on classical regression rate modeling in hybrid rockets, AIAA-2020-3758, 2020.

Marxman, G., and Gilbert, M., Turbulent boundary layer combustion in the hybrid rocket, Ninth symposium on combustion, Academic Press, New York, 1963, pp. 371-383.

Pistrone, D., Approaches to low fuel regression rate in hybrid rocket engines, International Journal of Aerospace Engineering (Hindawi Publishing Corporation), Vol. 2012, 2012 (Article ID 649753).

Sundaram, D.S., Puri, P., and Yang, V., A general theory of ignition and combustion of nano- and micron-sized alumnum particles, COnmbustion and Flame, Vol. 169, pp. 94-109, 2016.

Surmacz, P., and Rarata, G., Hybrid rocket development and application, MSc. Thesis Project, Institute of Aviation, 2009

Swami, R.D., and Gany, A., Analysis and testing of similarity and scale effects in hybrid rocket motors, Acta Astronautica, Vol. 52, pp. 619-628, 2003.

Whitmore, S.A., Peterson, Z.W., and Eilers, S.D., Comparing hydroxyl terminated polybutadiene and acrylonitrile butadiene styrene as hybrid fuels, J. Propulsion and Power, Vol. 29, No. 3, May-June 2013.

Woolridge, C.E., and Muzzy, R.J., Internal ballistic considerations in hybrid rocket design, J. Spacecraft and Rockets, Vol. 4, No. 2, pp. 255-262, 1967.